Published in final edited form as:
Metabolism. 2008 August ; 57(8): 1115–1124. doi:10.1016/j.metabol.2008.03.017.

Proteomic Analysis of Fructose-Induced Fatty Liver in Hamsters

Lihe Zhang, **German Perdomo**, **Dae Hyun Kim**, **Shen Qu**, **Steven Ringquist**, **Massimo Trucco**, and **H. Henry Dong***
Rangos Research Center, Division of Immunogenetics, Department of Pediatrics, Children's Hospital of Pittsburgh, University of Pittsburgh School of Medicine, Pittsburgh, PA 15213

Abstract

High fructose consumption is associated with the development of fatty liver and dyslipidemia with poorly understood mechanisms. We employed a MALDI-based proteomics approach to define the molecular events that link high fructose consumption to fatty liver in hamsters. Hamsters fed high fructose diet for 8 weeks, as opposed to regular chow-fed controls, developed hyperinsulinemia and hyperlipidemia. High fructose-fed hamsters exhibited fat accumulation in liver. Hamsters were sacrificed, and liver tissues were subjected to MALDI-based proteomics. This approach identified a number of proteins whose expression levels were altered by >2-fold in response to high fructose feeding. These proteins fall into five different categories including **1**) functions in fatty acid metabolism such as fatty acid binding protein and carbamoyl-phosphate synthase, **2**) proteins in cholesterol and triglyceride metabolism such as apolipoprotein A1 and protein disulfide isomerase, **3**) molecular chaperones such as GroEL, peroxiredoxin 2 and heat shock protein 70, whose functions are important for protein folding and anti-oxidation, **4**) enzymes in fructose catabolism such as fructose-1,6-bisphosphatase and glycerol kinase, and **5**) proteins with house-keeping functions such as albumin. These data provide insight into the molecular basis linking fructose-induced metabolic shift to the development of metabolic syndrome characterized by hepatic steatosis and dyslipidemia.

Keywords

Fatty liver; Dyslipidemia; Proteomics; Hamsters

Introduction

Fructose, which occurs naturally in honey and sweet fruits, is produced in crystalline and syrup forms for commercial use. The most commonly used corn syrup contains about 55% free fructose, and its use as a sweetener in processed foods and soft drinks has greatly increased by 20–30% over the past 20 years, a rate of increase similar to the incidence of obesity that has risen dramatically over the same period of time (1). Preclinical studies indicate that high fructose consumption is associated with the development of metabolic syndrome, as manifested by glucose intolerance, hyperinsulinemia, hypertriglyceridemia and whole body insulin resistance (2–6). In addition, there are some clinical data indicating that excessive fructose consumption for a limited period of time predisposes healthy subjects to body weight gain with concurrent elevation in plasma triglyceride and cholesterol levels, an atherogenic lipid profile

*Correspondence should be addressed to: Dr. Dong, Rangos Research Center, Children's Hospital of Pittsburgh, 3460 5th Avenue, Rm 5140, Pittsburgh, PA 15213, Tel: +1 (412) 692-6324, Fax: +1 (412) 692-5809, Email: dongh@pitt.edu.

that constitutes a major risk factor for clogging the artery and causing cardiovascular disease (7–10). Based on epidemiologic studies of obesity in relation to increased per capital consumption of high fructose corn syrup from beverages, it is thought that excessive dietary intake of fructose is a confounding factor for the increased prevalence of overweight and morbid obesity in industrial countries (1). There is evidence that frequent consumption of sugar-sweetened soft drinks is a potential contributing factor for childhood obesity (11–14).

Such detrimental effect of fructose on health can be ascribed to the metabolic pathway in which fructose is metabolized following its dietary intake. In this regard, fructose differs from glucose in three fundamental ways. First, after absorption in the gastrointestinal track, fructose fluxes via the portal circulation into the liver, where it is almost completely metabolized (15). Unlike glucose that enters hepatocytes through glucose transporter 2 (Glut2), fructose enters hepatocytes via glucose transporter 5 (Glut5) independently of insulin (16). Second, glucose breakdown is negatively regulated by phosphofructokinase, a hepatic enzyme that regulates glycolysis in liver, whereas fructose can evade this rate-limiting control mechanism and is metabolized into glycerol-3-phosphate and acetyl-CoA. These two intermediate metabolites serve as substrates for glyceride synthesis, contributing to very low-density lipoprotein (VLDL)-triglyceride (TG) production in liver (2,3). Third, fructose, as opposed to glucose, does not directly stimulate pancreatic insulin release, due to the lack of Glut5 expression in β-cells (16). Postprandial insulin secretion is instrumental for modulating glucose metabolism in peripheral tissues and regulating energy balance via the central nervous system through both direct and indirect mechanisms to control food intake and body weight gain (17–20). However, such an energy balancing mechanism does not respond to dietary fructose uptake, due to the inability of fructose to elicit insulin release. As a consequence, increased fructose flux into hepatocytes results in unrestrained production of intermediate metabolites, which favors energy storage by promoting *de novo* lipogenesis in liver.

High fructose consumption is associated with hepatic steatosis, but with poorly understood mechanisms (2–4). To investigate the underlying mechanism of fructose-induced fatty liver, we employed MALDI-based proteomics approach to identify candidate molecules that link high fructose consumption to the pathogenesis of hepatic steatosis. Syrian gold hamsters were fed a high fructose diet (60% fructose, n=6) or regular chow (n=6) for 8 weeks. Hamsters fed on high fructose diet, as opposed to control hamsters on regular chow, exhibited abnormal lipid profiles with increased fat deposition in liver. At the end of 8-week treatment, hamsters were sacrificed and liver tissues were subjected to MALDI-based proteomics. We show that high fructose feeding was associated with significant alterations in the expression of hepatic enzymes in multiple pathways. In addition to marked up-regulation of hepatic functions that promotes triglyceride synthesis and VLDL-TG production in liver, high fructose consumption resulted in perturbations in hepatic expression of anti-oxidant functions and molecular chaperones in protein folding. These data provide new insight into the molecular basis that links fructose-induced metabolic shift to aberrant hepatic metabolism in the pathogenesis of dyslipidemia and steatosis.

Materials and Methods

Animal studies

Male Syrian golden hamsters (5 week old, body weight, 81–90 g, Charles River Laboratory, Wilmington, MA) were fed with regular rodent chow or high fructose diet (60% fructose, DYET #161506, Dyets Inc., Bethlehem, PA) *ad libitum* in sterile cages with a 12-h light/dark cycle for 8 weeks. Blood was collected from tail vein into capillary tubes pre-coated with potassium-EDTA (Sarstedt, Nümbrecht, Germany) for preparation of plasma or determination of blood glucose levels using Glucometer Elite (Bayer, IN). Plasma triglyceride (TG) and cholesterol levels were determined using TG and cholesterol reagents (Thermo Electron,

Melbourne, Australia). Plasma non-esterified fatty acid (NEFA) levels were determined using the Wako NEFA assay kit (Wako Chemical USA, Richmond, VA). Plasma insulin levels were determined by anti-human insulin ELISA that cross-reacts with hamster insulin (ALPCO, Windham, NH). Plasma HDL cholesterol levels were determined using a cardiocheck analyzer (Polymer Technology System Inc. Indianapolis, IN). Plasma non-HDL cholesterol levels were calculated as total plasma cholesterol levels minus HDL cholesterol levels. At the end of 8-wk study, hamsters were sacrificed, and liver tissues were frozen in liquid N_2. All procedures were approved by the Institutional Animal Care and Use Committee (IACUC) of the Children's Hospital of Pittsburgh.

Glucose tolerance test

Hamsters were fasted for 5 h and injected intraperitoneally with 50% dextrose solution (Abbott Laboratories) at 5 g/kg body wt. Blood glucose levels were determined and plotted as a function of time. Area under the curve (AUC) of blood glucose profiles was calculated using the KaleidaGraph software (Synergy Software, Reading, PA). AUC values are inversely correlated with the ability of hamsters to dispose intraperitoneally injected glucose.

Hepatic lipid content

40 mg of liver tissue was homogenized in 800 μl of HPLC grade acetone. After incubation with agitation at room temperature overnight, aliquots (50 μl) of acetone-extract lipid suspension were used for the determination of TG concentrations using TG reagent (Thermo Electron). Hepatic lipid content was defined as mg of TG per gram of liver tissue.

Liver histology

Liver tissue from euthanized animals was fixed in Histoprep tissue embedding media (Fisher scientific, Hanover Park, IL) and snap frozen for fat staining with Oil red O (21).

Liver protein extraction

Aliquots of liver tissue (40 mg) were homogenized in 800 μl of M-PER buffer supplemented with 8-μl protease inhibitor cocktail (Pierce). Hepatic protein extracts were obtained after centrifugation at 13,000 rpm for 10 min in a microfuge.

Two-dimensional fluorescence difference gel electrophoresis (2D-DIGE)

Control and high fructose diet liver protein samples containing 300 μg protein were precipitated by 2-D Clean-Up Kit (GE Healthcare) and dissolved in 90 μl lysis buffer (7 M Urea, 2 M Thiourea, 4% w/v CHAPS, 1% v/v Triton X-100, 10 mM DTT). Samples were mixed with 3 μl of 100 mM HEPES (pH 8.0). 30 μl of each sample were combined to create a mixed standard sample for Cy2 labeling. The standard sample was incubated with 1 nmole Cy2. The remaining aliquots of the control and high fructose diet samples were incubated with 1 nmole Cy3 or 1 nmole Cy5, respectively. Each labeling reaction was incubated in an ice-water bath for 20 min in dark. After incubation of samples 1 μl of quenching solution (5 M methylamine, pH 8.0) was added and the mixtures incubated on ice for an additional 30 min in dark. Samples were combined and mixed with 5 μl of IPG buffer and 300 μl lysis buffer. Samples were transferred to a 1.5 ml ultracentrifuge tube and centrifuged at 100,000×g for 20 min at 4 °C. The supernatant was applied to an IPG strip (pH 4–7, 24 cm) and incubated for 20 hours using low voltage (30 V) in an Ettan IPGphor II IEF system (GE Healthcare). Following incubation and rehydration of the IPG strip proteins were isoelectric focused at 300 V for 30 min, 500 V for 30 min, 1000 V for 1 hour, and 8000 V for 10 hours. After isoelectric focusing (IEF) the strip was equilibrated for 15 min with 10 ml of 1% w/v DTT containing equilibration buffer (2% w/v SDS, 50 mM Tris-HCl pH 8.8, 6 M Urea, 30% v/v Glycerol and 0.001% Bromophenol blue) and for 15 min with 10 ml of 2.5% w/v iodoacetamide (IAA) containing equilibration buffer. Second

dimension SDS-PAGE was performed by transferring the IPG strip to a 12.5% single-percentage gel (dimension 1 mm, 20 cm, 26 cm) and electrophoresed using an Ettan DALT six electrophoresis system (GE Healthcare) for about 18 hours at 10 °C.

Differential in-gel analysis (DIA)

2D-gels were scanned using a Typhoon 9400 variable mode imager (GE Healthcare). Imager settings used blue-excited fluorescence (488 nm) for Cy2, green-excited fluorescence (532 nm) for Cy3, and red-excited fluorescence (633 nm) for Cy5. Data analysis was performed using DeCyder differential analysis software, version 5.02 (GE Healthcare). Gel images were processed for spot detection and determination of the relative protein abundance based on fluorescence intensity, defined as spot volume. Changes in protein expression levels, expressed as spot volume ratios, were calculated after dividing the spot volume of a given protein at high fructose conditions by its spot volume at regular chow conditions. Protein spots were selected as up-regulated or down-regulated among those exceeding a 2-fold difference in fluorescence intensity. Differentially expressed proteins were manually spot-picked from Coomassie Blue G-250 (BIO-RAD) stained gels and gel plugs were transferred to 96-well collection plates.

In-gel digestion

Gel plugs were destained by washing twice with 100 µl of 50% methanol, 50 mM ammonium bicarbonate at room temperature and dehydrated with 100 µl of 100% acetonitrile for 20 min. Samples were transferred to 0.5 ml eppendorf tubes containing 20 µl of 100% acetonitrile and dried in a vacufuge (Eppendorf). Trypsin digestion was performed by addition of 12 µl of a 20 µg/ml trypsin solution (100 µM HCl, 25 mM ammonium bicarbonate, 10% acetonitrile) and incubated at 37°C overnight with gentle shaking. Supernatants were transferred to 0.5 ml eppendorf tubes and gel plugs were extracted twice at room temperature with 50 µl of 50% acetonitrile, 1% TFA for 1 hour each extraction. Extracts were combined with the supernatant and dried in a vacufuge at room temperature. Samples were stored overnight at −20°C.

Mass spectrometry

Dried peptides from in-gel digestion were dissolved in 3 µl of 50% acetonitrile, 0.3% TFA and mixed with 3 µl of freshly prepared matrix solution (10 mg/ml α-cyano-4-hydroxy-cinnamic acid in 50% acetonitrile, 0.3% TFA). The mixture, 0.6 µl, was spotted onto a MALDI plate (Applied Biosystems). The 4700 Proteomics Analyzer MALDI-TOF/TOF (Applied Biosystems) was used to identify proteins from the trypsin digest. Analysis of samples used reflector positive ion mode acquisition and processing method to collect peptide spectra in the mass range of 800–4000 Da. The ten highest intensity peptides were selected for MS/MS analysis using MS/MS mode acquisition with the 1kV positive ion and processing method. Data processing was performed with GPS Explorer Workstation (Applied Biosystems) and MASCOT database analysis of mammalian proteins.

Immunoblot assay

Aliquots (40 mg) of liver tissue were homogenized in 800 µl ice-cold M-PER solution (Pierce, Rockford, IL) supplemented with 8 µl of protease inhibitor cocktail (Pierce). Aliquots of 20 µg of protein lysates were resolved on 4–20% SDS-polyacrylamide gels and subjected to immunoblot assay using antibodies against chaperonin GroEL (catalog no. SPA-806F; Assay Designs/Stressgen Bioreagents, MI, USA), heat shock protein-70 (1:7,500 dilution, Cat #3095-100; Biovision, CA, USA), senescence marker protein-30 (1:1,000 dilution, sc-25951; Santa Cruz Biotechnology, CA, USA), protein disulfide isomerase (1:500 dilution, 539229; Calbiochem, CA, USA), fatty acid binding protein (1:15,000 dilution, NB200-434, Novus Biologicals, CO, USA), and apolipoprotein A–I (1:10,000 dilution, K23001R; Biodesign, ME, USA). Proteins were detected using the chemiluminescence western blotting reagents (Roche

Diagnostics, Indianapolis, IN, USA). The intensity of protein bands was quantified by densitometry using the NIH Image software (National Institutes of Health, Bethesda, MD) as described (22).

Statistics

Statistical analyses of data were performed by analysis of variance (ANOVA) using StatView software (Abacus Concepts, Inc., CA). ANOVA post hoc tests were performed to study the significance between high fructose and regular chow groups. Data were expressed as the mean ± SEM. P values < 0.05 were considered statistically significant.

Results and Discussion

Characteristics of hamsters on regular chow vs. high fructose diet

To study the effect of high fructose consumption on glucose and lipid metabolism, we randomly assigned 5-week male hamsters into two groups (n=6) to either regular chow or high fructose diet. After 8-week feeding, we determined blood glucose and lipid parameters. As shown in Table 1, high fructose-fed hamsters were associated with a slight body weight gain and a small increase in blood glucose levels. However, the differences in mean body weight and blood glucose levels between high fructose and regular chow groups did not reach a significant level, as determined by ANOVA. We also determined blood glucose profiles in response to intraperitoneal glucose challenge. Hamsters fed on high fructose diet displayed impaired glucose tolerance, as reflected in the increased AUC values in comparison to control hamsters (Table 1). This effect mirrored the significant elevation of plasma insulin levels, which were indicative of whole body insulin resistance in high fructose-fed hamsters. When plasma lipid profiles were analyzed, significantly higher levels of plasma NEFA, triglyceride and total cholesterol were detected in high fructose-fed hamsters. High fructose-fed hamsters also displayed elevated HDL cholesterol levels without significant alterations in non-LDL cholesterol levels, when compared to control hamsters. Furthermore, hamsters fed high fructose diet exhibited significantly higher levels of hepatic lipid content. In keeping with previous observations (3,4,6,23,24), high fructose consumption is associated with lipid disorders in rodents. To corroborate these findings, hamsters were sacrificed at the end of 8-week study, and liver tissues were subjected to fat staining. As shown in Fig. 1, hamsters fed high fructose diet were associated with increased fat deposition in liver.

Proteomic profiling of fructose-induced fatty liver

To gain insight into high fructose-induced lipid disorder, we subjected livers of high fructose-fed and control mice to MALDI-based proteomics, because liver is the major site for fructose catabolism. As show in Fig. 2 and Table 2, this approach identified a total of 33 protein spots whose expression levels were altered by >2-fold. These proteins fall into five different categories including 1) house-keeping functions such as albumin, ferritin heavy chain and actin, 2) molecular chaperones such as GroEL and heat shock protein 70 (Hsp70), whose functions are important for protein folding or stress, 3) enzymes in fructose catabolism such as fructose-1,6-bisphosphatase (FBPase) and glycerol kinase (Gyk), 4) functions in lipid metabolism such as fatty acid binding protein (FABP) and carbamoyl-phosphate synthase 1 (CPS1), and 5) proteins in cholesterol metabolism such as apolipoprotein A1 (apoA-1). To corroborate these findings, we subjected liver tissues from control and high fructose-fed hamsters to semi-quantitative immunoblot assay. As shown in Fig. 3, this assay confirmed the results obtained from proteomics studies. Thus, in accordance with lipid disorders in high fructose-fed hamsters, high fructose feeding resulted in significant alterations in the expression of proteins in hepatic metabolism. The physiological significance of these findings was discussed in relation to hepatic metabolism and steatosis below.

Hepatic proteins that were up-regulated in response to fructose feeding

In accordance with increased fat infiltration into liver, we detected a significant induction of fatty acid binding protein (FABP) in high fructose-fed hamsters (Table 2 and Fig. 3). FABP is a cytosolic fatty acid chaperone that plays a critical role in facilitating fatty acid uptake and intracellular transport in response to dietary signals, and regulating glucose and lipid metabolism. Hepatic FABP levels are also upregulated in response to high fat feeding or increased alcohol consumption, coinciding with the development of hepatic steatosis in mice (25,26). In contrast, genetic ablation of hepatic FABP gene protects against high fat-induced obesity and hepatic steatosis in mice (27–29). These data establish FABP as an important determinant of hepatic lipid composition and turnover, suggesting that high fructose-mediated induction of FABP production plays a causative role in increased fat deposition in livers of high fructose-fed hamster. In support of this view, we detected a significant elevation of plasma non-esterified fatty acid levels in high fructose-fed hamsters. In addition, Aoyama et al. (30) show that fructose is converted to fatty acids in liver at much greater rates than glucose. This effect, along with increased flux of fatty acids to liver, is thought to be a contributing factor for enhanced *de novo* lipogenesis in liver and elevated postprandial triglyceride levels in blood in response to increased dietary fructose uptake (3,7,10,31,32).

Protein disulfide isomerase (PDI) is an abundant multifunctional protein that resides in the lumen in the endoplasmic reticulum (ER). In response to high fructose feeding, hepatic PDI levels were markedly elevated (Table 2 and Fig. 3). PDI functions to promote disulfide bond formation, isomerization, and reduction within the ER. In addition, PDI is associated with chaperone activities that contribute to its ability to promote proper folding of newly synthesized proteins (33–35). In the ER, PDI forms a complex with microsomal triglyceride transfer protein (MTP) that catalyzes the transport of triglyceride, cholesteryl ester and phospholipid between microsomal membranes, a rate-limiting step for hepatic VLDL assembly and secretion (36, 37). Our proteomics-based approach did not pick up MTP protein, due to its relatively lower abundance in liver. However, using immunoblot assay, we and others have previously shown that hepatic MTP production was increased in hamsters in response to high fructose feeding (3,6,23,24). This effect parallels fructose-mediated induction of PDI expression in liver, accounting in part for increased hepatic VLDL-TG production and contributing to the pathogenesis of hypertriglyceridemia in high fructose-fed hamsters (2,3,23,38).

In response to high fructose feeding, hepatic production of apolipoprotein A1 (apoA-1) were markedly increased (Table 2 and Fig. 3). Abundantly expressed in liver, apoA-1 is a major component of HDL and plays an important role in plasma cholesterol metabolism (39). ApoA-1 is necessary for the formation of nascent HDL, known as pre-β HDL that acts as the acceptor of cholesterol in HDL maturation (40,41). This effect accounts for its ability to promote reverse cholesterol transport, a dynamic process in which HDL uptakes cholesterol from peripheral tissue including macrophages for subsequent delivery to liver for excretion (42,43). Reverse cholesterol transport is thought to be an important anti-atherogenic mechanism for protecting against the development of atherosclerosis (42,44). Interestingly, elevated apoA-1 production mirrors the increase in plasma HDL levels in high fructose-induced hyperlipidemic hamsters. Likewise, Guren et al (45) show that plasma HDL cholesterol and apoA-1 levels were elevated in obese and diabetic mice with altered lipid metabolism. Fructose-mediated induction of hepatic apoA-1 production may serve as a compensatory mechanism for increased cholesterol catabolism, as both total and HDL cholesterol levels were significantly elevated in response to high fructose feeding (Table 1).

Interestingly, we detected a marked induction of Peroxiredoxin 2 (PrxII), coinciding with increased fat deposition in livers of high fructose-fed hamsters (Table 2). This effect is accompanied by induction of the antioxidant enzyme, glutathione S-transferase (GST) in livers in response to high fructose feeding (Table 2). PrxII is member of the mammalian

peroxiredoxin family of thiol proteins that play important roles in antioxidant defense. Expressed abundantly in liver, PrxII gene encodes a cytosolic peroxidase that functions to eliminate endogenous H_2O_2 generated from metabolism, which helps protect cells from oxidative stress and apoptosis (46,47). Significant induction of PrxII also develops in alcohol-fed mouse livers (48). These results raise the possibility that high fructose or alcohol consumption exerts a deleterious effect on hepatic metabolism and liver function. Fructose-mediated induction of PrxII might serve as a compensatory mechanism to alleviate the oxidant damage caused by inappropriately increased fructose catabolism in liver. In support of this notion, PrxII is abundantly expressed in liver and is markedly induced in response to ischemia/reperfusion injury during liver transplantation (49,50). This effect has been viewed as a cytoprotective mechanism to protect liver from oxidative damage and preserve liver function post-transplantation (49,50).

In addition, two hepatic enzymes, glycerol kinase (GyK) and fructose-1-,6-biphosphatase (FBPase) in glucose metabolism, were increased in response to high fructose feeding. GyK phosphorylates glycerol to glycerol 3-phosphate, a source for dihydroxyacetone phosphate, glycerolipids, glucose, glycogen and protein (51). FBPase is an important gluconeogenic enzyme that catalyses the hydrolysis of fructose 1,6-bisphosphate to fructose 6-phosphate and Pi (52). Furthermore, hepatic levels of malate dehydrogenase (MDH) were also increased in response to high fructose feeding (Table 2). MDH is an enzyme of the tricarboxylic acid cycle that converts malate and NAD into oxaloacetate and NADH, playing important roles in hepatic gluconeogenesis (53). A potential mechanism of augmented hepatic production of GyK, FBPase and MDH is to accommodate increased fructose catabolism and favor energy storage in high fructose-fed hamsters (Table 2).

Leucyl aminopeptidase (LAP) is another hepatic enzyme that is up-regulated in response to high fructose feeding (Table 2). LAP plays an important role in glutathione metabolism and in the degradation of glutathione S-conjugates (54,55). The physiological significance underlying fructose-mediated induction of LAP production in liver remains to be determined. In addition, we detected a significant increase in hepatic production of albumin, coinciding with the increase of plasma non-esterified fatty acids in high fructose-fed hamsters (Table 2). These results are consistent with the property of serum albumin to bind and transport fatty acids in the circulation (56).

Hepatic proteins that were down-regulated in response to fructose feeding

Carbamoyl-phosphate synthase 1 (CPS1) is among hepatic proteins that were down-regulated by increased fructose consumption. CPS1 is abundantly expressed in liver and catalyzing the rate-limiting step in the urea cycle, a metabolic pathway that is primarily responsible for removing waste nitrogen from the body (57). Hepatic deficiency of CSP1 affects the ability of liver to remove waste nitrogen, resulting in severe hyperammonemia (57). To date, there is little information regarding the regulation of CPS1 expression in liver. Inoue et al. (58) reported that genetic disruption of hepatic CCAAT/enhancer-binding protein alpha (C/EBPα) resulted in hepatic CPS1 deficiency, suggesting that CPS1 expression is regulated by C/EBPα in liver. We detected 2–4 folds of reduction in hepatic CPS1 protein levels in high fructose-fed hamsters, correlating with increased fat infiltration in liver (Table 2). These results presage an association between CPS1 deficiency and hepatic steatosis in high fructose-fed hamsters. In support of this notion, C/EBPα null mice with inheritable CPS1 deficiency also develop age-dependent hepatic steatosis (58).

High fructose feeding also resulted in >3-fold reduction in the expression levels of 10-formyltetrahydrofolate dehydrogenase (FDH) (Table 2). FDH is a high-affinity folate-binding protein that catalyzes the $NADP^+$-dependent conversion of 10-formyltetrahydrofolate to CO_2 and tetrahydrofolate (59,60). Expressed mainly in liver and brain (61–63), FDH functions

to regulate the folate-mediated one-carbon metabolism (60). Mice with chronic ethanol consumption are associated with significantly reduced hepatic FDH activity, accompanied by folate deficiency and liver weight gain (64). The physiological significance of hepatic FDH deficiency, resulting from high fructose or chronic ethanol consumption, remains to be determined.

We also show that senescence marker protein 30 (SMP30) expression in liver was significantly down-regulated by 3.5-fold in response to high fructose feeding (Table 2 and Fig. 3). SMP30 is a 34-kDa protein that is abundantly expressed in liver, lung and kidney, and its expression levels decrease with aging (65). SMP30 is a lactone-hydrolyzing enzyme for biosynthesis of l-ascorbic acid, an intermediary metabolite that is involved in long-chain fatty acid metabolism in liver (66). SMP30 knockout mice exhibit abnormal accumulations of triglycerides, cholesterol, and phospholipids, accompanied by an increased mortality rate (65,67). Hepatic SMP30 levels were markedly reduced in high fat-induced obese mice with metabolic abnormalities including hypercholesterolemia and hepatic steatosis (68). These data together with our present studies suggest a close association that links increased fructose feeding to SMP30 deficiency, lipid disorders and aging. Interestingly, there is evidence that chronic fructose consumption promotes the formation of advanced glycation end products and accelerates several age-related variables in male rats (69,70). Further studies are needed to characterize the function of SMP30 in lipid metabolism and glycation for better understanding the underlying mechanism of lipid abnormality associated with SMP30 down-regulation in liver or its potential role in aging.

Ferretins are expressed abundantly in liver and spleen, and are responsible for iron storage. Recently, Rashid et al. (71) show that ferretins interact physically with apolipoproatein B (apoB) in the liver. In a follow-up study, Hevi et al. (72) demonstrate that ferretins bind specifically to apoB and inhibit apoB secretion from cultured HepG2 cells. There is clinical evidence that a human subject with familial hypobetalipoproteinemia exhibits hepatic steatosis and liver dysfunction, accompanied by marked deposition of iron in the liver (73). Although the underlying mechanism of ferritin-mediated inhibition of hepatic apoB secretion remains to be elucidated, the available data in the literature suggest a physiological linkage between iron storage and lipid metabolism, as hepatic apoB plays a rate-limiting role in regulating triglyceride-rich VLDL production in the liver. Consistent with this notion, we show that hepatic expression of ferritins were reduced, correlating inversely with elevated apoB and VLDL secretion in high fructose-fed hamsters, as reported by Taghibiglou et al. (74,75).

In addition to its deleterious effect on lipid metabolism, there are preclinical studies indicating that high fructose consumption is associated with oxidative stress. Rats fed a high fructose diet exhibit increased lipid oxidation, accompanied by reduced expression of anti-oxidant enzymes such as superoxide dismutase (SOD) and glutathione peroxidase (GPx) in liver and heart (76–79). High fructose consumption also increases free radical production in rats (79,80). Interestingly, dietary supplementation of antioxidants such as vitamin E, which mitigates oxidative stress and suppresses free radical production, ameliorates fructose-induced insulin resistance and hyperlipidemia in rats (80,81). These data illustrate a close association between fructose-elicited oxidative stress and the development of metabolic disorders.

It is noteworthy that Morand et al. (82) have used a similar proteomics approach to probe the molecular basis underlying fructose-induced hepatic insulin resistance and metabolic dyslipidemia in the hamster model. Their studies focus on the proteomic profiling of hepatic endoplasmic reticulum (ER)-associated proteins, demonstrating that high fructose consumption is associated with dysreglation of ER resident chaperones including ER60, ERp46, ERp29, PDI and GRP94 in the liver of hamsters after 2 weeks of high fructose feeding. These ER resident proteins play important role in protein folding and lipoprotein secretion.

These findings together with our present data suggest that unrestrained fructose influx into the liver result in perturbation of multiple pathways in hepatic metabolism, contributing to hepatic insulin resistance and dyslipidemia in high fructose-fed animals.

Conclusion

Excessive fructose consumption is associated with dyslipidemia, culminating in markedly elevated lipid levels in plasma and increased fat deposition in liver. Our studies provide insight into the underlying mechanism of fructose-induced hepatic steatosis and diabetic dyslipidemia. We show that high fructose feeding resulted in significant alterations in multiple pathways in hepatic metabolism. These include: 1) functions in fatty acid transportation, VLDL-TG assembly and cholesterol metabolism, 2) molecular chaperones in protein folding in the ER, 3) anti-oxidant functions in cytoprotective mechanism, and 4) enzymes for the accommodation of fructose catabolism in response to increased fructose influx into liver. These perturbations in hepatic enzyme expressions are consistent with the idea that high fructose consumption exerts a deleterious effect on hepatic metabolism, contributing to enhanced *de novo* lipogenesis, augmented VLDL-TG secretion and the development of dyslipidemia (2–4,10,83). While increased consumption of fructose-rich sweeteners in soft drinks is considered a contributing factor for the prevalence of obesity in industrial countries (7,8,84), our studies support the idea of limiting excessive fructose addition in beverages to counteract the epidemic of obesity and type 2 diabetes (1,84).

Acknowledgements

We thank Drs. Adama Kamagate and Sandra Slusher for critical reading of this manuscript. This study was supported in part National Health Institute grants DK066301 (HHD) and Autoimmunity Centers of Excellence U19-AI056374-01 (SR and MT), and Department of Defense ERMS #00035010 (SR and MT).

References

1. Bray GA, Nielsen SJ, Popkin BM. Consumption of high-fructose corn syrup in beverages may play a role in the epidemic of obesity. Am J Clin Nutr 2004;79:537–543. [PubMed: 15051594]
2. Basciano H, Federico L, Adeli K. Fructose, insulin resistance, and metabolic dyslipidemia. Nutr Metab (Lond) 2005;2:5. [PubMed: 15723702]
3. Qu S, Su D, Altomonte J, et al. PPAR{alpha} mediates the hypolipidemic action of fibrates by antagonizing FoxO1. Am J Physiol Endocrinol Metab 2007;292:E421–E434. [PubMed: 16985262]
4. Jurgens H, Haass W, Castaneda TR, et al. Consuming fructose-sweetened beverages increases body adiposity in mice. Obes Res 2005;13:1146–1156. [PubMed: 16076983]
5. Avramoglu RK, Qiu W, Adeli K. Mechanisms of metabolic dyslipidemia in insulin resistant states: deregulation of hepatic and intestinal lipoprotein secretion. Front Biosci 2003;8:d464–d476. [PubMed: 12456312]
6. Taghibiglou C, Carpentier A, Van Iderstine SC, et al. Mechanisms of hepatic very low density lipoprotein overproduction in insulin resistance. Evidence for enhanced lipoprotein assembly, reduced intracellular ApoB degradation, and increased microsomal triglyceride transfer protein in a fructose-fed hamster model. J Biol Chem 2000;275:8416–8425. [PubMed: 10722675]
7. Teff KL, Elliott SS, Tschop M, et al. Dietary fructose reduces circulating insulin and leptin, attenuates postprandial suppression of ghrelin, and increases triglycerides in women. J Clin Endocrinol Metab 2004;89:2963–2972. [PubMed: 15181085]
8. Elliott SS, Keim NL, Stern JS, et al. Fructose, weight gain, and the insulin resistance syndrome. Am J Clin Nutr 2002;76:911–922. [PubMed: 12399260]
9. Kohen-Avramoglu R, Theriault A, Adeli K. Emergence of the metabolic syndrome in childhood: an epidemiological overview and mechanistic link to dyslipidemia. Clin Biochem 2003;36:413–420. [PubMed: 12951167]

10. Bantle JP, Raatz SK, Thomas W, et al. Effects of dietary fructose on plasma lipids in healthy subjects. Am J Clin Nutr 2000;72:1128–1134. [PubMed: 11063439]
11. Ludwig DS, Peterson KE, Gortmaker SL. Relation between consumption of sugar-sweetened drinks and childhood obesity: a prospective, observational analysis. Lancet 2001;357:505–508. [PubMed: 11229668]
12. James J, Kerr D. Prevention of childhood obesity by reducing soft drinks. International journal of obesity (2005) 2005;29:S54–S57. [PubMed: 16385753]
13. Philippas NG, Lo CW. Childhood obesity: etiology, prevention, and treatment. Nutr Clin Care 2005;8:77–88. [PubMed: 16013226]
14. Gibson SA. Associations between energy density and macronutrient composition in the diets of pre-school children: sugars vs. starch. Int J Obes Relat Metab Disord 2000;24:633–638. [PubMed: 10849587]
15. Smith LH Jr, Ettinger RH, Seligson D. A comparison of the metabolism of fructose and glucose in hepatic disease and diabetes mellitus. J Clin Invest 1953;32:273–282. [PubMed: 13052684]
16. Sato Y, Ito T, Udaka N, et al. Immunohistochemical localization of facilitated-diffusion glucose transporters in rat pancreatic islets. Tissue & cell 1996;28:637–643. [PubMed: 9004533]
17. Schwartz MW, Porte D Jr. Diabetes, obesity, and the brain. Science 2005;307:375–379. [PubMed: 15662002]
18. Schwartz MW, Woods SC, Porte D Jr, et al. Central nervous system control of food intake. Nature 2000;404:661–671. [PubMed: 10766253]
19. Havel PJ. Control of energy homeostasis and insulin action by adipocyte hormones: leptin, acylation stimulating protein, and adiponectin. Curr Opin Lipidol 2002;13:51–59. [PubMed: 11790963]
20. Woods SC, Porte D Jr, Bobbioni E, et al. Insulin: its relationship to the central nervous system and to the control of food intake and body weight. Am J Clin Nutr 1985;42:1063–1071. [PubMed: 3904396]
21. Dong H, Altomonte J, Morral N, et al. Basal insulin gene expression significantly improves conventional insulin therapy in type 1 diabetic rats. Diabetes 2002;51:130–138. [PubMed: 11756332]
22. Qu S, Altomonte J, Perdomo G, et al. Aberrant Forkhead box O1 function is associated with impaired hepatic metabolism. Endocrinology 2006;147:5641–5652. [PubMed: 16997836]
23. Carpentier A, Taghibiglou C, Leung N, et al. Ameliorated hepatic insulin resistance is associated with normalization of microsomal triglyceride transfer protein expression and reduction in very low density lipoprotein assembly and secretion in the fructose-fed hamster. J Biol Chem 2002;277:28795–28802. [PubMed: 12048212]
24. Chong T, Naples M, Federico L, et al. Effect of rosuvastatin on hepatic production of apolipoprotein B-containing lipoproteins in an animal model of insulin resistance and metabolic dyslipidemia. Atherosclerosis 2006;185:21–31. [PubMed: 16002078]
25. Hoekstra M, Stitzinger M, van Wanrooij EJ, et al. Microarray analysis indicates an important role for FABP5 and putative novel FABPs on a Western-type diet. J Lipid Res 2006;47:2198–2207. [PubMed: 16885566]
26. Lieber CS. Alcoholic fatty liver: its pathogenesis and mechanism of progression to inflammation and fibrosis. Alcohol 2004;34:9–19. [PubMed: 15670660]
27. Newberry EP, Xie Y, Kennedy SM, et al. Protection against Western diet-induced obesity and hepatic steatosis in liver fatty acid-binding protein knockout mice. Hepatology 2006;44:1191–1205. [PubMed: 17058218]
28. Spann NJ, Kang S, Li AC, et al. Coordinate transcriptional repression of liver fatty acid-binding protein and microsomal triglyceride transfer protein blocks hepatic very low density lipoprotein secretion without hepatosteatosis. J Biol Chem 2006;281:33066–33077. [PubMed: 16950764]
29. Cao H, Maeda K, Gorgun CZ, et al. Regulation of metabolic responses by adipocyte/macrophage Fatty Acid-binding proteins in leptin-deficient mice. Diabetes 2006;55:1915–1922. [PubMed: 16804058]
30. Aoyama Y, Yoshida A, Ashida K. Effect of dietary fats and fatty acids on the liver lipid accumulation induced by feeding a protein-repletion diet containing fructose to protein-depleted rats. J Nutr 1974;104:741–746. [PubMed: 4830279]

31. Mayes PA. Intermediary metabolism of fructose. Am J Clin Nutr 1993;58:754S–765S. [PubMed: 8213607]
32. Hallfrisch J. Metabolic effects of dietary fructose. Faseb J 1990;4:2652–2660. [PubMed: 2189777]
33. Wetterau JR, Combs KA, McLean LR, et al. Protein disulfide isomerase appears necessary to maintain the catalytically active structure of the microsomal triglyceride transfer protein. Biochemistry 1991;30:9728–9735. [PubMed: 1911761]
34. Wetterau JR, Aggerbeck LP, Laplaud PM, et al. Structural properties of the microsomal triglyceride-transfer protein complex. Biochemistry 1991;30:4406–4412. [PubMed: 2021632]
35. Satoh M, Shimada A, Kashiwai A, et al. Differential cooperative enzymatic activities of protein disulfide isomerase family in protein folding. Cell Stress Chaperones 2005;10:211–220. [PubMed: 16184766]
36. Berriot-Varoqueaux N, Aggerbeck LP, Samson-Bouma M, et al. The role of the microsomal triglygeride transfer protein in abetalipoproteinemia. Annu Rev Nutr 2000;20:663–697. [PubMed: 10940349]
37. Hussain MM, Shi J, Dreizen P. Microsomal triglyceride transfer protein and its role in apoB-lipoprotein assembly. J Lipid Res 2003;44:22–32. [PubMed: 12518019]
38. Guo Q, Wang PR, Milot DP, et al. Regulation of lipid metabolism and gene expression by fenofibrate in hamsters. Biochim Biophys Acta 2001;1533:220–232. [PubMed: 11731332]
39. Barter PJ, Rye KA. The rationale for using apoA-I as a clinical marker of cardiovascular risk. J Intern Med 2006;259:447–454. [PubMed: 16629850]
40. Chau P, Nakamura Y, Fielding CJ, et al. Mechanism of prebeta-HDL formation and activation. Biochemistry 2006;45:3981–3987. [PubMed: 16548525]
41. Rye KA, Barter PJ. Formation and metabolism of prebeta-migrating, lipid-poor apolipoprotein A–I. Arterioscler Thromb Vasc Biol 2004;24:421–428. [PubMed: 14592845]
42. Lewis GF, Rader DJ. New insights into the regulation of HDL metabolism and reverse cholesterol transport. Circ Res 2005;96:1221–1232. [PubMed: 15976321]
43. Stein O, Ben-Naim M, Dabach Y, et al. Macrophage cholesterol efflux to free apoprotein A–I in C3H and C57BL/6 mice. Biochem Biophys Res Commun 2002;290:1376–1381. [PubMed: 11820773]
44. Tangirala RK, Tsukamoto K, Chun SH, et al. Regression of atherosclerosis induced by liver-directed gene transfer of apolipoprotein A–I in mice. Circulation 1999;100:1816–1822. [PubMed: 10534470]
45. Gruen ML, Plummer MR, Zhang W, et al. Persistence of high density lipoprotein particles in obese mice lacking apolipoprotein A–I. J Lipid Res 2005;46:2007–2014. [PubMed: 15995171]
46. Low FM, Hampton MB, Peskin AV, et al. Peroxiredoxin 2 functions as a noncatalytic scavenger of low-level hydrogen peroxide in the erythrocyte. Blood 2007;109:2611–2617. [PubMed: 17105810]
47. Yang CS, Lee DS, Song CH, et al. Roles of peroxiredoxin II in the regulation of proinflammatory responses to LPS and protection against endotoxin-induced lethal shock. J Exp Med 2007;204:583–594. [PubMed: 17325201]
48. Kim BJ, Hood BL, Aragon RA, et al. Increased oxidation and degradation of cytosolic proteins in alcohol-exposed mouse liver and hepatoma cells. Proteomics 2006;6:1250–1260. [PubMed: 16408314]
49. Shau H, Merino A, Chen L, et al. Induction of peroxiredoxins in transplanted livers and demonstration of their in vitro cytoprotection activity. Antioxid Redox Signal 2000;2:347–354. [PubMed: 11229538]
50. Cesaratto L, Vascotto C, D'Ambrosio C, et al. Overoxidation of peroxiredoxins as an immediate and sensitive marker of oxidative stress in HepG2 cells and its application to the redox effects induced by ischemia/reperfusion in human liver. Free Radic Res 2005;39:255–268. [PubMed: 15788230]
51. Herzog B, Waltner-Law M, Scott DK, et al. Characterization of the human liver fructose-1,6-bisphosphatase gene promoter. Biochem J 2000;351(Pt 2):385–392. [PubMed: 11023824]
52. Lamont BJ, Visinoni S, Fam BC, et al. Expression of human fructose-1,6-bisphosphatase in the liver of transgenic mice results in increased glycerol gluconeogenesis. Endocrinology 2006;147:2764–2772. [PubMed: 16497803]

53. Kondo H, Minegishi Y, Komine Y, et al. Differential regulation of intestinal lipid metabolism-related genes in obesity-resistant A/J vs. obesity-prone C57BL/6J mice. Am J Physiol Endocrinol Metab 2006;291:E1092–E1099. [PubMed: 16822957]
54. Josch C, Klotz LO, Sies H. Identification of cytosolic leucyl aminopeptidase (EC 3.4.11.1) as the major cysteinylglycine-hydrolysing activity in rat liver. Biol Chem 2003;384:213–218. [PubMed: 12675513]
55. Cappiello M, Lazzarotti A, Buono F, et al. New role for leucyl aminopeptidase in glutathione turnover. Biochem J 2004;378:35–44. [PubMed: 14583094]
56. Curry S, Brick P, Franks NP. Fatty acid binding to human serum albumin: new insights from crystallographic studies. Biochim Biophys Acta 1999;1441:131–140. [PubMed: 10570241]
57. Summar ML, Hall L, Christman B, et al. Environmentally determined genetic expression: clinical correlates with molecular variants of carbamyl phosphate synthetase I. Mol Genet Metab 2004;81:S12–S19. [PubMed: 15050969]
58. Inoue Y, Inoue J, Lambert G, et al. Disruption of hepatic C/EBPalpha results in impaired glucose tolerance and age-dependent hepatosteatosis. J Biol Chem 2004;279:44740–44748. [PubMed: 15292250]
59. Tsybovsky Y, Donato H, Krupenko NI, et al. Crystal structures of the carboxyl terminal domain of rat 10-formyltetrahydrofolate dehydrogenase: implications for the catalytic mechanism of aldehyde dehydrogenases. Biochemistry 2007;46:2917–2929. [PubMed: 17302434]
60. Anguera MC, Field MS, Perry C, et al. Regulation of folate-mediated one-carbon metabolism by 10-formyltetrahydrofolate dehydrogenase. J Biol Chem 2006;281:18335–18342. [PubMed: 16627483]
61. Min H, Shane B, Stokstad EL. Identification of 10-formyltetrahydrofolate dehydrogenase-hydrolase as a major folate binding protein in liver cytosol. Biochim Biophys Acta 1988;967:348–353. [PubMed: 3196754]
62. Neymeyer VR, Tephly TR. Detection and quantification of 10-formyltetrahydrofolate dehydrogenase (10-FTHFDH) in rat retina, optic nerve, and brain. Life Sci 1994;54:PL395–PL399. [PubMed: 8177005]
63. Neymeyer V, Tephly TR, Miller MW. Folate and 10-formyltetrahydrofolate dehydrogenase (FDH) expression in the central nervous system of the mature rat. Brain Res 1997;766:195–204. [PubMed: 9359603]
64. Min H, Im ES, Seo JS, et al. Effects of chronic ethanol ingestion and folate deficiency on the activity of 10-formyltetrahydrofolate dehydrogenase in rat liver. Alcohol Clin Exp Res 2005;29:2188–2193. [PubMed: 16385189]
65. Maruyama N, Ishigami A, Kuramoto M, et al. Senescence marker protein-30 knockout mouse as an aging model. Ann N Y Acad Sci 2004;1019:383–387. [PubMed: 15247050]
66. Kondo Y, Inai Y, Sato Y, et al. Senescence marker protein 30 functions as gluconolactonase in L-ascorbic acid biosynthesis, and its knockout mice are prone to scurvy. Proc Natl Acad Sci U S A 2006;103:5723–5728. [PubMed: 16585534]
67. Ishigami A, Kondo Y, Nanba R, et al. SMP30 deficiency in mice causes an accumulation of neutral lipids and phospholipids in the liver and shortens the life span. Biochem Biophys Res Commun 2004;315:575–580. [PubMed: 14975739]
68. Park JY, Seong JK, Paik YK. Proteomic analysis of diet-induced hypercholesterolemic mice. Proteomics 2004;4:514–523. [PubMed: 14760724]
69. Levi B, Werman MJ. Long-term fructose consumption accelerates glycation and several age-related variables in male rats. J Nutr 1998;128:1442–1449. [PubMed: 9732303]
70. Mikulikova K, Eckhardt A, Kunes J, et al. Advanced glycation end-product pentosidine accumulates in various tissues of rats with high fructose intake. Physiol Res. 2007
71. Rashid KA, Hevi S, Chen Y, et al. A proteomic approach identifies proteins in hepatocytes that bind nascent apolipoprotein B. J Biol Chem 2002;277:22010–22017. [PubMed: 11934886]
72. Hevi S, Chuck SL. Ferritins can regulate the secretion of apolipoprotein B. J Biol Chem 2003;278:31924–31929. [PubMed: 12813058]
73. Whitfield AJ, Barrett PH, Robertson K, et al. Liver dysfunction and steatosis in familial hypobetalipoproteinemia. Clin Chem 2005;51:266–269. [PubMed: 15514099]

74. Taghibiglou C, Van Iderstine SC, Kulinski A, et al. Intracellular mechanisms mediating the inhibition of apoB-containing lipoprotein synthesis and secretion in HepG2 cells by avasimibe (CI-1011), a novel acyl-coenzyme A: cholesterol acyltransferase (ACAT) inhibitor. Biochemical pharmacology 2002;63:349–360. [PubMed: 11853686]

75. Taghibiglou C, Rashid-Kolvear F, Van Iderstine SC, et al. Hepatic very low density lipoprotein-ApoB overproduction is associated with attenuated hepatic insulin signaling and overexpression of protein-tyrosine phosphatase 1B in a fructose-fed hamster model of insulin resistance. J Biol Chem 2002;277:793–803. [PubMed: 11598116]

76. Fields M, Ferretti RJ, Reiser S, et al. The severity of copper deficiency in rats is determined by the type of dietary carbohydrate. Proceedings of the Society for Experimental Biology and Medicine Society for Experimental Biology and Medicine (New York, NY 1984;175:530–537.

77. Busserolles J, Rock E, Gueux E, et al. Short-term consumption of a high-sucrose diet has a pro-oxidant effect in rats. The British journal of nutrition 2002;87:337–342. [PubMed: 12064343]

78. Busserolles J, Zimowska W, Rock E, et al. Rats fed a high sucrose diet have altered heart antioxidant enzyme activity and gene expression. Life Sci 2002;71:1303–1312. [PubMed: 12106595]

79. Busserolles J, Gueux E, Rock E, et al. High fructose feeding of magnesium deficient rats is associated with increased plasma triglyceride concentration and increased oxidative stress. Magnes Res 2003;16:7–12. [PubMed: 12735477]

80. Busserolles J, Gueux E, Rock E, et al. Substituting honey for refined carbohydrates protects rats from hypertriglyceridemic and prooxidative effects of fructose. J Nutr 2002;132:3379–3382. [PubMed: 12421854]

81. Faure P, Rossini E, Lafond JL, et al. Vitamin E improves the free radical defense system potential and insulin sensitivity of rats fed high fructose diets. J Nutr 1997;127:103–107. [PubMed: 9040552]

82. Morand JP, Macri J, Adeli K. Proteomic profiling of hepatic endoplasmic reticulum-associated proteins in an animal model of insulin resistance and metabolic dyslipidemia. J Biol Chem 2005;280:17626–17633. [PubMed: 15760893]

83. Ostos MA, Recalde D, Baroukh N, et al. Fructose intake increases hyperlipidemia and modifies apolipoprotein expression in apolipoprotein AI-CIII-AIV transgenic mice. J Nutr 2002;132:918–923. [PubMed: 11983814]

84. Raben A, Vasilaras TH, Moller AC, et al. Sucrose compared with artificial sweeteners: different effects on ad libitum food intake and body weight after 10 wk of supplementation in overweight subjects. Am J Clin Nutr 2002;76:721–729. [PubMed: 12324283]

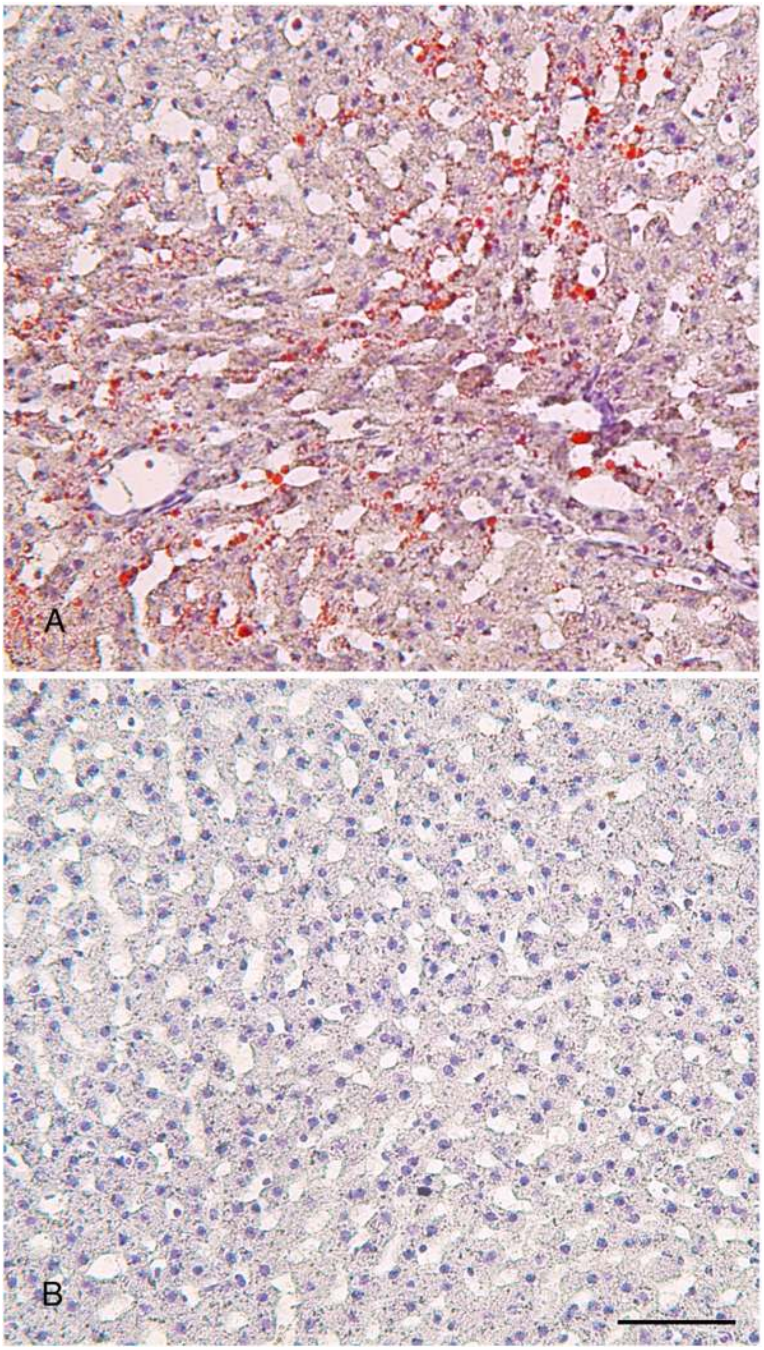

Fig. 1.

Hepatic lipid content. Hamsters were sacrificed after 8 weeks of feeding on high fructose diet or regular chow. Liver tissues of hamsters treated with high fructose (**A**) and regular chow (**B**) were embedded with Histoprep tissue embedding media. Frozen sections (8 μm) were cut and stained with Oil red O, followed by counterstaining with hematoxylin. Bar=50 μm.

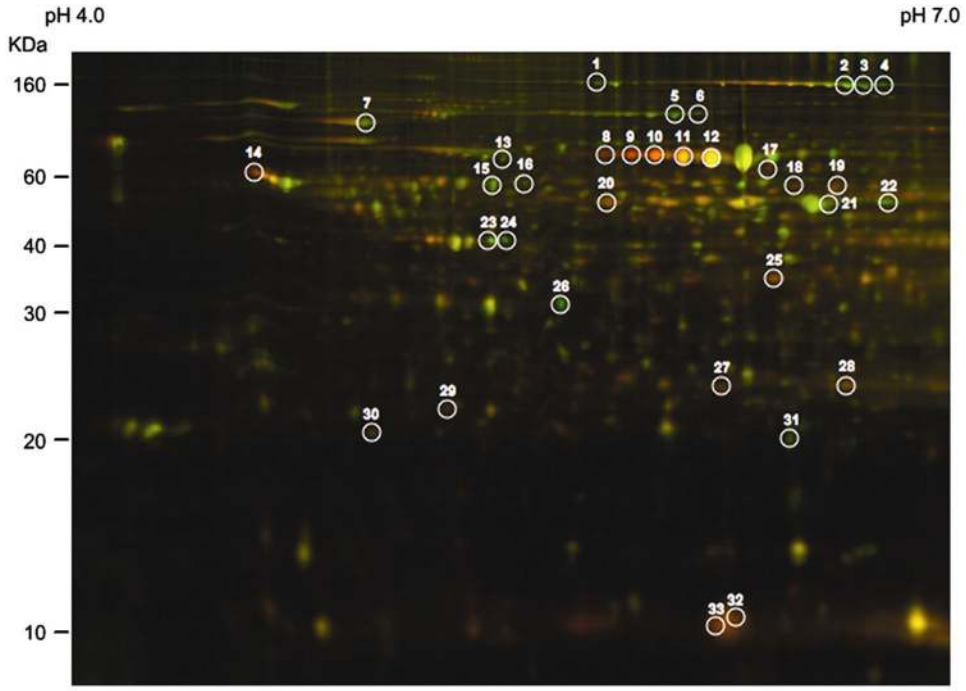

Fig. 2.

2-D DIGE analysis of liver proteins. In the 2-D gel image, hepatic proteins of hamsters on regular chow were shown in green color, whereas hepatic proteins of hamsters on high fructose diet were shown in red color. Protein spots of greater than 2-fold differences between control and high fructose groups were cut out and subjected to mass spectrometry for the identification of protein ID.

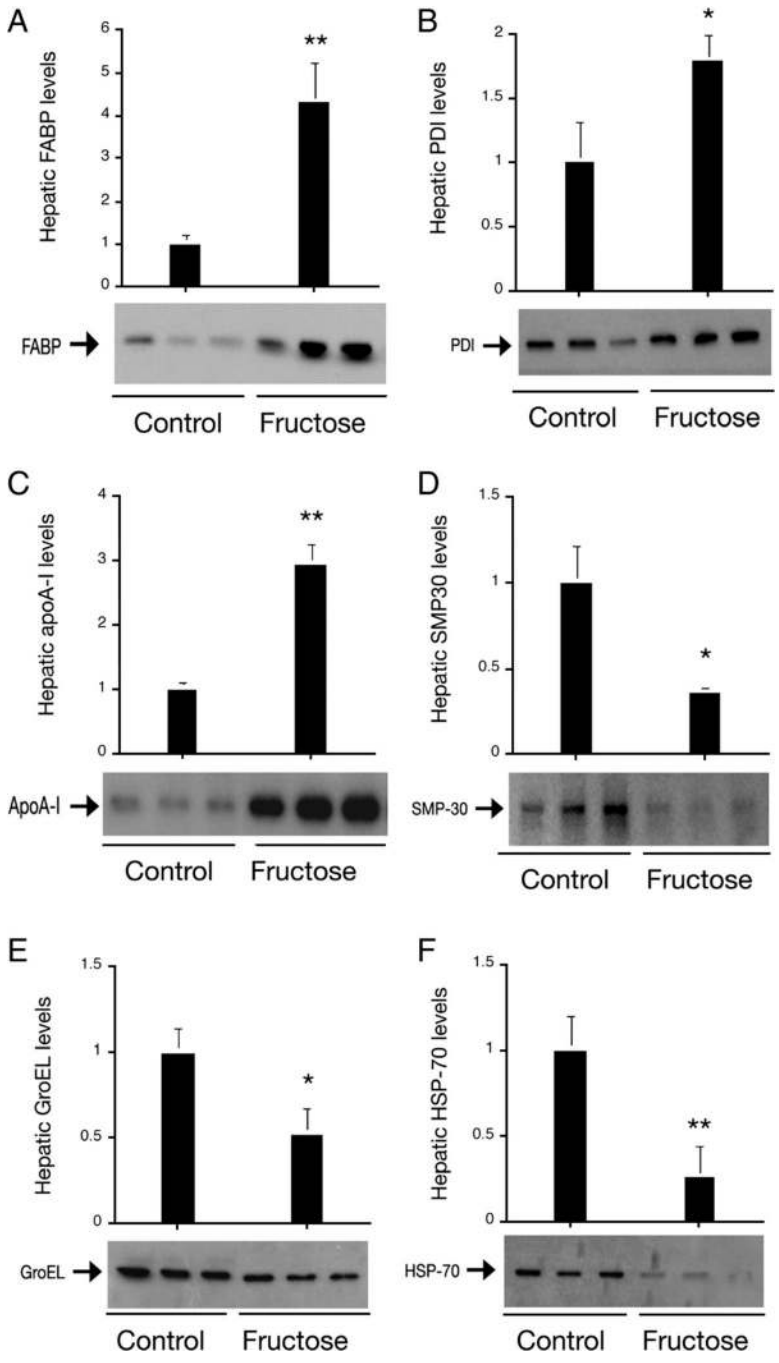

Fig. 3.

Immunoblot analysis of liver proteins. Aliquots of liver tissues (40 mg) from control and high fructose-fed hamsters were homogenized and a fixed amount of liver proteins (20 μg) were subjected to semi-quantitative immunoblot assay using antibodies against fatty acid binding protein (A), protein disulfide isomerase (B), and apolipoprotein A–I (C), senescence marker protein-30 (D), chaperonin GroEL (E), and heat shock protein-70 (F). *P<0.05. **P<0.005 vs. controls.

Table 1

Characteristics of hamsters fed on regular chow vs. high fructose diet

	Regular chow	High fructose
Body weight (g)	134±4.5	142±7.8
Blood glucose (mg/dL)	86±12	101±7
AUC (arbitrary unit)	1.0±0.09	1.7±0.13*
Plasma insulin (μU/mL)	0.17±0.03	0.73±0.13*
Plasma NEFA (mEq/L)	0.15±0.01	0.39±0.06*
Plasma triglyceride (mg/dL)	175±20	388±50*
Plasma cholesterol (mg/dL)	149±13	194±16*
Plasma HDL-c (mg/dL)	117±8	151±5*
Plasma non-HDL-c (mg/dL)	31±8	35±5
Hepatic lipid content (mg/g liver)	6.3±0.3	10.7±0.8*

Hamsters were fed regular chow or high fructose diet for 8 weeks, followed by the determination of body weight, fasting blood glucose levels, fasting plasma levels of insulin, FFA, triglyceride, cholesterol, HDL-cholesterol (HDL-c). Non-HDL-cholesterol (non-HDL-c) levels were calculated by subtracting HDL-c from total cholesterol levels in plasma. Glucose tolerance was performed after 7 weeks of fructose feeding for the determination of AUC of blood glucose profiles in response to glucose challenge. Hamsters were sacrificed at the end of study and liver tissues were used for the determination of hepatic lipid content, defined as mg of triglyceride per gram of wet liver tissue.

*$P<0.05$ vs. control by ANOVA.

Table 2

Hepatic proteins with >2-fold alterations in response to high fructose feeding

Spot No.	Protein ID	Accession No.	Molecul ar mass	pI value	Score	Pattern of regulation	Volume ratio	*P* values
1	Carbamoylphosphate synthase 1	SYRTCA	164,475	6.33	444	Down	−2.13	0.05
2	Carbamoylphosphate synthase 1	SYRTCA	164,475	6.33	573	Down	−2.51	0.87
3	Carbamoylphosphate synthase 1	SYRTCA	164,475	6.33	547	Down	−4.81	0.026
4	Carbamoylphosphate synthase 1	SYRTCA	164,475	6.33	397	Down	−4.16	0.028
5	10-formyltetrahydrofolate dehydrogenase	A60560	99,015	5.61	600	Down	−3.48	0.00003
6	10-formyltetrahydrofolate dehydrogenase	A60560	99,015	5.61	292	Down	−3.64	0.0013
7	Heat shock protein 70	Q9DC41	72,378	5.01	1220	Down	−2.14	0.047
8	Albumin 1	Q8C7C7	64,960	5.49	110	Up	4.66	0.0023
9	Albumin 1	Q8C7C7	64,960	5.49	173	Up	5.84	0.00018
10	Albumin 1	Q8C7C7	64,960	5.49	140	Up	5.39	0.00079
11	Albumin 1	Q8C7C7	64,960	5.49	143	Up	4.07	0.00015
12	Albumin 1	Q8C7C7	64,960	5.49	179	Up	2.79	0.02
13	Annexin VI	S01786	75,838	5.34	560	Down	−2.15	0.017
14	Protein disulfide-isomerase	Q8R4U2	56,974	4.78	419	Up	2.77	0.16
15	Chaperonin groEL	HHMS60	60,903	5.91	1050	Down	−2.28	0.25
16	BC027197 NID	AAH27197	54,014	5.69	272	Down	−2.19	0.0028
17	Malate dehydrogenase	Q921S3	63,957	6.87	132	Up	3.76	0.012
18	Aldehyde dehydrogenase class 1 member B1	Q9CZS1	57,516	6.59	260	Up	2.85	0.42
19	Leucine aminopeptidase	Q99P44	56,105	7.62	279	Up	2.10	0.17
20	Glycerol kinase	Q8C2M1	60,522	5.47	277	Up	2.04	0.0047
21	Aldehyde dehydrogenase class 2	I48966	56,501	7.53	704	Down	−2.16	0.78
22	Aldehyde dehydrogenase calss 2	I48966	56,501	7.53	302	Down	−3.00	0.049
23	Actin	Q61276	41,666	5.21	348	Down	−2.25	0.0004
24	Actin	Q61276	41,666	5.21	231	Down	−2.71	0.0005
25	Fructose-1,6-bisphosphatase	1BK4A	34,129	7.71	67	Up	2.34	0.0059
26	Senescence marker protein-30	Q7TSW4	33,224	5.41	89	Down	−3.55	0.0003
27	Glutathione S-transferase	S33860	25,953	7.71	97	Up	2.20	0.1
28	Glutathione S-transferase	S33860	25,953	7.71	247	Up	2.16	0.013
29	Apolipoprotein A1	Q9Z2L4	30,719	5.86	363	Up	3.35	0.0013
30	Peroxiredoxin 2	Q8K3U7	21,799	5.35	326	Up	3.07	0.00005
31	Ferritin heavy chain	FRIH_CRIGR	21,341	5.73	241	Down	−3.86	0.1
32	Fatty acid binding protein	A32640	10,173	5.88	58	Up	3.01	0.000001
33	Fatty acid binding protein	A32640	10,173	5.88	66	Up	2.93	0.00006

Proteomic profiling of livers of hamsters fed on high fructose (n=6) and regular chow (n=6) were performed. Determination of changes in protein expression levels was performed on a total of 12 2-D gels from individual hamster livers in control and fructose_groups, using DeCyder software version 5 and calculated from the volume ratios of the normalized fluorescent signals. Protein spots with significant differences of greater than 2 fold ($P<0.05$) between high fructose- and regular chow-fed hamsters were identified. All identified proteins match the apparent molecular mass and pI values, based on the 2-D gels.